

Human and Monkey Fetal Brain Development of the Supramammillary-Hippocampal Projections: A System Involved in the Regulation of Theta Activity

BRIGITTE BERGER,^{1*} MONIQUE ESCLAPEZ,² CHANTAL ALVAREZ,¹
GUNDELA MEYER,³ AND MARTIN CATALA⁴

¹INSERM U106, Hôpital Salpêtrière, 75651 Paris cedex 13, France

²INMED, INSERM U29, Luminy, B.P.13, 13273 Marseille cedex 09, France

³Department of Anatomy, Faculty of Medicine, University La Laguna, 38071 Tenerife, Spain

⁴Service d'Histologie, Embryologie et Cytogénétique, UMR CNRS 7000, CHU Pitié-Salpêtrière (AP-HP, Université Paris 6), Paris, France

ABSTRACT

The supramammillary (SUM)-hippocampal pathway plays a central role in the regulation of theta rhythm frequency. We followed its prenatal development in eight *Cynomolgus* monkeys (*Macaca fascicularis*) from embryonic day E88 to postnatal day 12 (term 165 days) and in eight human fetuses from 17.5 to 40 gestational weeks, relying on neurochemical criteria established in the adult (Nitsch and Leranth [1993] *Neuroscience* 55:797–812). We found that 1) SUM afferents reached the dentate juxtgranular and CA2 pyramidal cell layers at midgestation in human fetuses, earlier than in monkeys (two-thirds of gestation [E109]). They co-expressed calretinin, substance P, and acetylcholinesterase but not γ -aminobutyric acid (GABA) or glutamic acid decarboxylase (GAD); 2) the presumed parent neurons in the monkey SUM expressed calretinin or both calretinin and substance P; 3) most of them were surrounded by GAD-containing terminals that might correspond to the septo-SUM feedback pathway (Leranth et al. [1999] *Neuroscience* 88:701); and 4) in addition, a large band of calretinin-labeled terminals that did not co-express substance P, GAD, or acetylcholinesterase was present in the deepest one-third of the dentate molecular layer in both the *Cynomolgus* monkey and human fetuses. It persisted in the adult monkey but not in adult human hippocampus; it remains questionable whether it originates in the SUM. In conclusion, the early ingrowth of the excitatory SUM-hippocampal system in human and non-human primates may contribute to the prenatal activity-dependent development of the hippocampal formation. The possibility and the functional importance of an in utero generation of hippocampal theta-like activity should also be considered. *J. Comp. Neurol.* 429:515–529, 2001. © 2001 Wiley-Liss, Inc.

Indexing terms: dentate gyrus; calretinin; substance P; GABA; GAD; primate

Extensive anatomical and electrophysiological studies in adult rodents have revealed the central role played by the projections from the supramammillary nucleus (SUM), a caudal hypothalamic cell group, to the hippocampo-septal complex (Haglund et al., 1984; Saper, 1985; Vertes, 1992; Kirk and McNaughton, 1993; Kocsis and Vertes, 1994; McNaughton et al., 1995; Kirk et al., 1996; Vertes and Kocsis, 1997; Leranth et al., 1999). They form a main component of the so-called ascending brainstem hippocampal synchronizing system (Vertes and Koc-

sis 1997; Bland and Oddie, 1998). As such, they participate in the complex anatomical loop involved in the

Grant sponsor: INSERM U106; Grant number: 237 6900.

*Correspondence to: B. Berger, INSERM U106, Hôpital Salpêtrière, 47 Bld. de l'Hôpital, 75651, Paris cedex 13, France.
E-mail: bberger@infobiogen.fr

Received 29 June 2000; Revised 31 August 2000; Accepted 25 September 2000

genesis and control of hippocampal theta activity, which is considered to serve a critical role in processes of synaptic plasticity and mnemonic functions (Holscher et al., 1997; Vertes and Kocsis 1997; Bland and Oddie, 1998; Thomas et al., 1998; Klimesch, 1999; Perez et al., 1999). Actually, the frequency of hippocampal theta activity is primarily determined in the SUM (Kirk and McNaughton, 1993; Kocsis and Vertes, 1994; McNaughton et al., 1995; Bland and Oddie, 1998; Kirk, 1998). In rat pups, both theta rhythmic waves and membrane potential oscillations generated in the theta frequency range occur at the end of the first postnatal week (Leblanc and Bland, 1979; Konopacki et al., 1988; Strata, 1998) or even earlier (Psarropoulou and Avoli, 1995).

Similar rhythms have been demonstrated in adult human and nonhuman primates (Crowne and Radcliffe, 1975; Watanabe and Niki, 1985; Meador et al., 1991; Stewart and Fox, 1991; Eifuku et al., 1995; Kahana et al., 1999; Klimesch, 1999; Tesche and Karhu, 2000). The developmental time course of this oscillatory activity and of its presumed anatomical substrate in primates has not been determined.

The SUM-hippocampal system has already been identified in the adult monkey by combined immunocytochemical, lesion, and tracing studies (Veazy et al., 1982a,b; Nitsch and Leranth, 1993, 1994; Seress et al., 1993; Leranth and Nitsch, 1994). The topographical and neurochemical characteristics of these pathways indicated that an anatomic-chemical identification would be possible in fetal brains without tracing the connections. We have used this approach for comparing the development of this system in monkey and human fetuses. In adult monkeys, the SUM projections to the hippocampal formation end selectively in the molecular layer of the dentate gyrus at the juxtgranular level and in the CA2 pyramidal cell layer (Veazy et al., 1982a,b). A calretinin and substance P innervation of extrinsic origin has been described in these areas (Nitsch and Leranth, 1993, 1994; Seress et al., 1993; Leranth and Nitsch, 1994), and these two markers were found to be co-localized in their parent cell bodies in the SUM. These neurons did not contain γ -aminobutyric acid (GABA)ergic markers (GABA or glutamic acid decarboxylase [GAD], the GABA-synthetic enzyme) and were considered to exert excitatory effects. Combined histochemical and tracing studies also revealed the presence of acetylcholinesterase (AChE) in the soma of the SUM-hippocampal projecting neurons (Bakst and Amaral, 1984). Accordingly, AChE activity appeared indeed more prominent in the inner third of the dentate molecular layer and in the CA2 field than in other areas (Bakst and Amaral, 1984; Alonso and Amaral, 1995).

Beside these morphological studies in adult monkeys, recent experiments in adult rodents have specified the neurochemical and ultrastructural characteristics of another component of the theta activity-related anatomical loop, the septo-SUM pathway (Swanson and Cowan, 1979). This pathway originates mainly from calretinin-containing GABAergic neurons and forms multiple perisomatic contacts on the SUM neurons that give issue to the hippocampal projections (Borhegyi and Freund, 1998; Leranth et al., 1999).

The goals of this study were therefore 1) to identify and specify the developmental time course of the SUM-hippocampal system in fetal monkeys, by using the aforementioned topographical and neurochemical criteria com-

pleted by co-localization studies at the level of the dentate and ammonic terminals; 2) to visualize, at the SUM level, the axon terminals corresponding presumably to the septo-SUM system; and 3) to perform a comparative study in human fetuses, for further evaluation of the extent to which the monkey brain, particularly that of Old World monkey, may be considered a valuable model for the prenatal development of the human brain.

MATERIALS AND METHODS

Animals and fixation

Eight cynomolgus monkeys (*Macaca fascicularis*) ranging in age from embryonic day E88 (term 165 days) to postnatal day 12 (PN12) were obtained from the breeding colony of the INRA Primate Center at Jouy en Josas. This series included 88-, 109-, 127-, 136-, 142-, 147-, and 156-day-old fetal animals, one of each age delivered by cesarean section under anesthesia with ketamine HCl 10 mg/kg and diazepam 1 mg/kg. Several of them were used in previous studies (Berger et al., 1997, 1999). An adult 4-year-old monkey was provided by the Institut Pasteur (Paris). The study was conducted under the approval and guidelines of the Ethical Committee of the Primate Center. All animals were anesthetized with ketamine HCl 10 mg/kg and perfused transcardially with cold 4% or 2% paraformaldehyde in 0.1 M phosphate buffer, pH 7.3, following a brief flush with 0.9% NaCl. After a 30-minute perfusion, the brain was removed and sectioned in the coronal plane, and the slices were postfixed for 4–6 hours in the same fixative. They were cryoprotected by immersion in 10% and then 20% phosphate-buffered sucrose and frozen at -50°C in isopentane cooled with dry ice.

Human brains

Samples of eight human fetal brains were available for this study. All brains came from spontaneous or medically

Fig. 1. Calretinin (CR) and substance P (SP) labeling patterns in coronal sections of the monkey fetal hippocampus at E83 (A), E88 (B), and E109 (C–G). **A:** The main finding in the context of this study is the absence of CR-labeled terminals in the target areas of the SUM-hippocampal projections along the granular cell layer (arrows) of the dentate gyrus (DG) and in the pyramidal cell layer of CA2. CR-labeled nonpyramidal neurons are numerous at the hilar border of the DG granular layer, in the stratum oriens (so), and in the pyramidal cell layer of CA1. Spindle-shaped Cajal-Retzius cells are distributed along the obliterated hippocampal fissure (hf) in CA3 and the subpial layer of the DG (Berger and Alvarez, 1996). CR-immunoreactive fibers run in the alveus (al). **B:** SP-labeled terminals are also lacking in the target layers of the SUM-hippocampal projections (arrows). Numerous SP-immunoreactive nonpyramidal neurons are present in the stratum oriens (so). A large fascicle of SP-containing fibers courses through the molecular layer of CA1 and CA2. **C:** Dense CR immunolabeling (arrow) is observed in the deep molecular layer (mol) of the latero-caudal limb of the dentate gyrus (DG). **D:** A network of CR-labeled fibers (arrow) occupies the pyramidal cell layer (py) of CA2. so, stratum oriens; sr, stratum radiatum. **E:** High magnification reveals the accumulation of CR-immunoreactive terminals in the dentate outermost granular and juxtgranular cell layers. gl, granular cell layer; mol, molecular layer. **F:** A thin band of SP-labeled terminals occupies the dentate juxtgranular layer (arrow). A dense SP-labeled innervation is observed in CA2. DG, dentate gyrus; gl, granular layer. **G:** Higher magnification confirms that the density of the SP-labeled innervation in the dentate juxtgranular layer is lighter than the density of calretinin-containing terminals (compare G with E). gl, granular layer; mol, molecular layer. Scale bars = 100 μm in A–C,F; 40 μm in D; 30 μm in E,G.

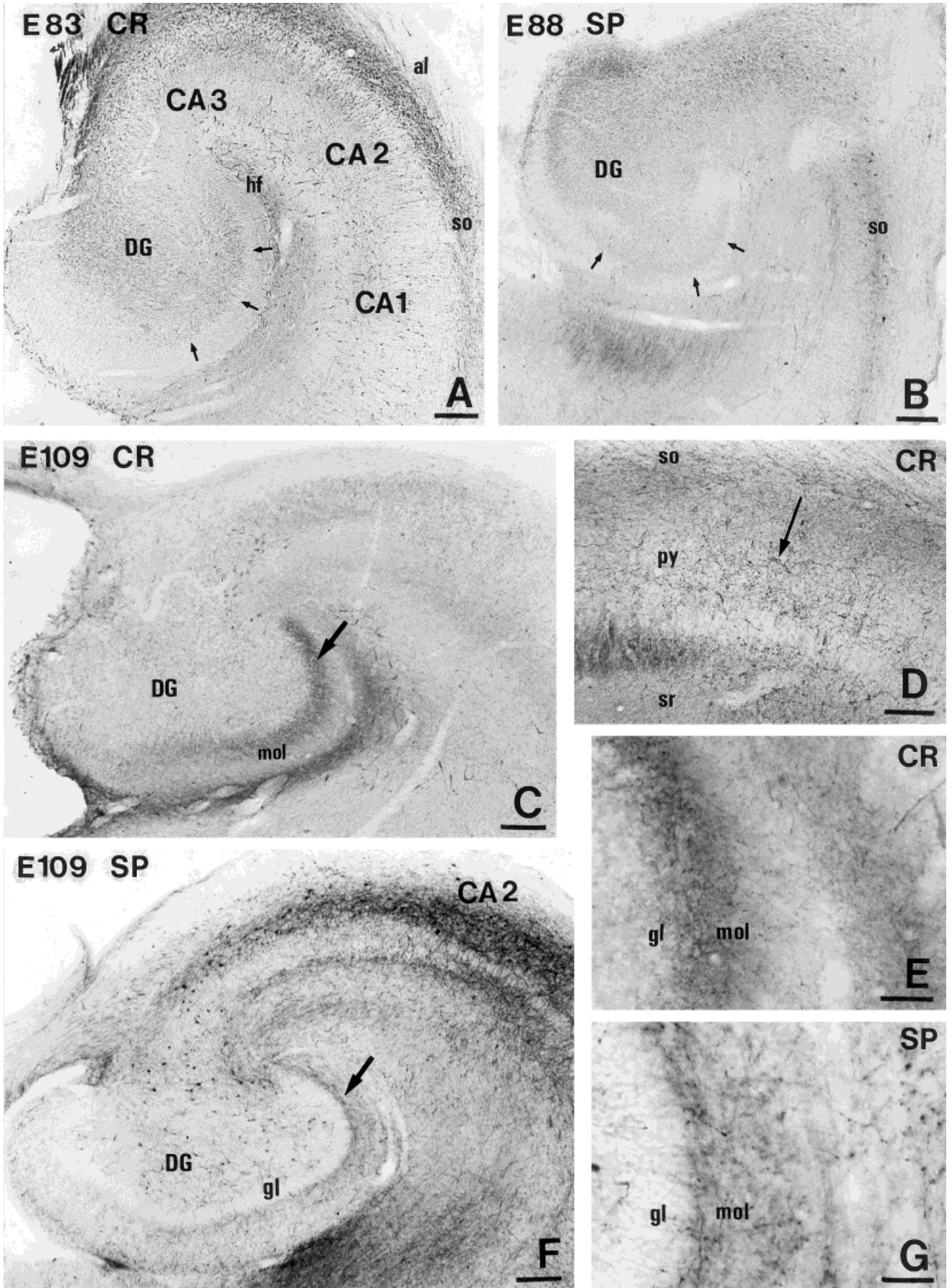


Figure 1

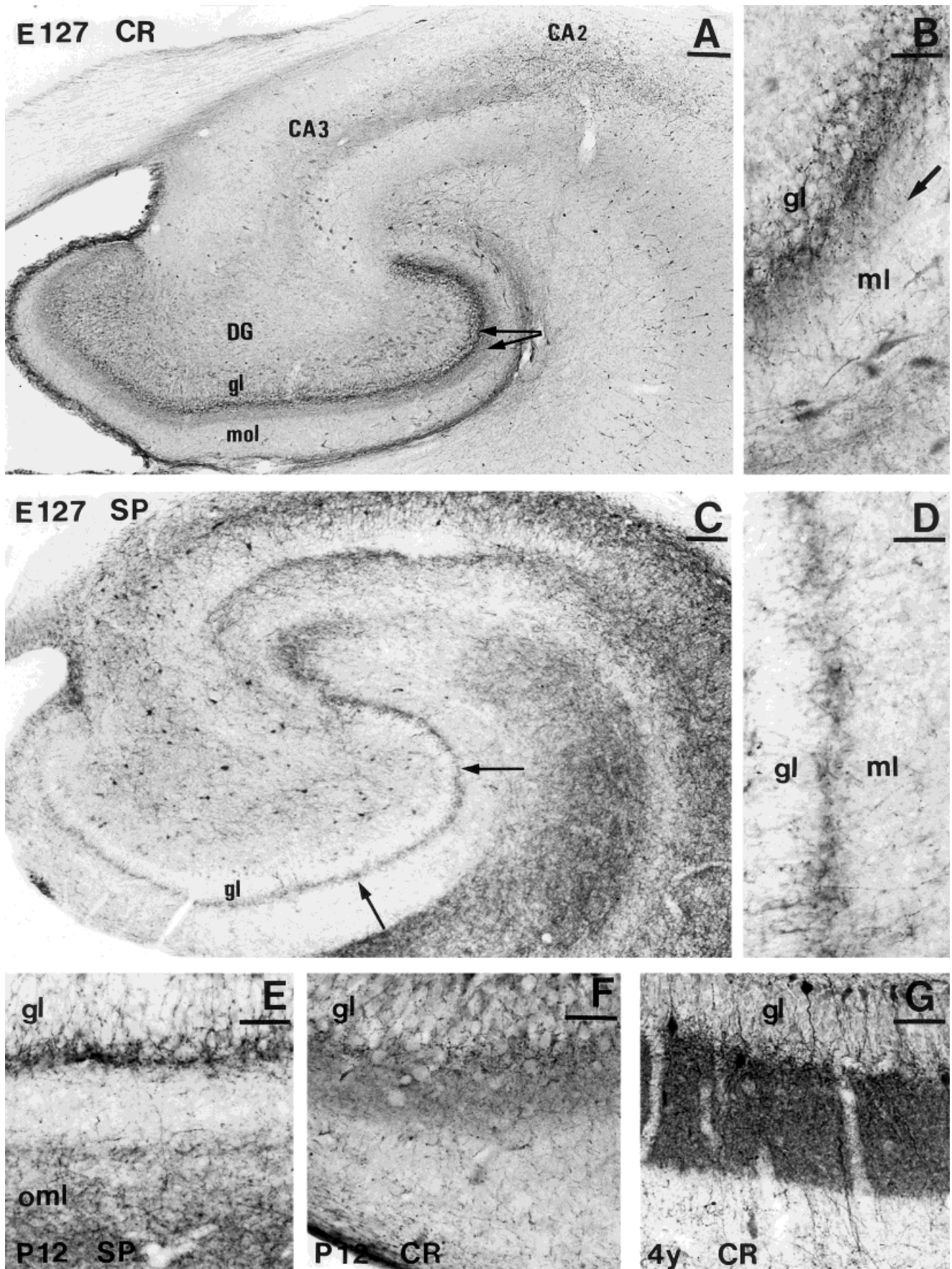


Figure 2

indicated abortions, according to the guidelines of the French National Committee for Health and Life Sciences and of the Ethical Committee of the University Hospital La Laguna. The gestational age of each fetus was estimated by menstrual history and fetal measurements. Five of these brains of 20 (2), 23, 24, and 32.5 gestational weeks (GW) were obtained from the Unit of Fetal Pathology of the CHU Pitié-Salpêtrière within 4–24 hours after termination of pregnancy. Blocks of the hippocampus at the midbody or caudal levels were fixed by immersion in cold 4% paraformaldehyde in 0.1 M phosphate buffer, pH 7.3, for 10–24 hours, except for the older brain, which was left for several months in formalin 10%. They were then processed and frozen like the monkey brains. Routine pathological analysis revealed no evidence of malformation or other abnormalities in these fetal brains. A few 10- μ m-thick paraffin sections of the hippocampal formation from three other brains, fixed in Bouin's fixative (17.5 GW and 40 GW [2]), were available from the Department of Anatomy, Faculty of Medicine of the University of Laguna, Tenerife, Spain. Calretinin-stained sections of the hippocampal formation from two normal brains (a 41-year-old adult male and a 15-year-old girl) were also examined.

Immunocytochemistry

Free-floating 30–48- μ m-thick sections, according to the age of the monkey fetal brain, were obtained on a freezing microtome and processed for Nissl staining and immunocytochemistry. Frozen human brain samples were cut 15–20 μ m thick on a cryostat.

Antibodies

Calretinin was labeled by using a polyclonal antibody (Schwaller et al., 1993; Swant, Bellinzona, Switzerland) raised in rabbit or in goat, according to the requirements of single or double immunohistochemical staining. GAD65 was localized with the monoclonal antibody GAD-6, raised

in mice by Chang and Gottlieb (1988), GAD67 with the rabbit polyclonal antiserum K2 obtained by Kaufman et al. (1991), GABA with an antibody generated in rabbit (Sigma, St. Louis, MO), substance P with a monoclonal antibody raised in rat (Harlan Sera-Lab, Belton, Loughborough, UK), and AChE with a monoclonal antibody raised in mouse (Chemicon, Temecula, CA).

Single immunohistochemical staining

The sections were incubated for 36 hours at 4°C with the primary antibody (calretinin 1:10,000–1:40,000; SP 1:2,000) diluted in 0.02 M phosphate-buffered saline (PBS) containing 0.02% gelatin, 0.25% Triton X-100, and 8% human serum albumin. The antibody was detected with the corresponding streptavidin biotin-peroxidase system (Amersham, Little Chalfont, UK). Diaminobenzidine (DAB; 0.05%) with 0.005% H₂O₂ in 0.02 M PBS buffer, pH 7.3, was used as the chromogen. Labeling of substance P was intensified by using DAB (0.02%) with 0.6% nickel ammonium sulfate and 0.003% H₂O₂ in 0.05 M Tris buffer, pH 7.6. Paraffin and cryostat sections obtained from the long formalin-fixed brain were pretreated in a microwave prior to incubation. The sections were transferred into 0.01 M sodium citrate buffer, pH 6, and irradiated in a microwave oven (Samsung) at 750 W for 10 minutes (Werner et al., 1996).

Double immunohistochemical labeling

The following primary and secondary antibodies were used:

1. For the dual immunodetection of calretinin and GAD65, calretinin and substance P, or calretinin and AChE, simultaneous incubation with calretinin antibody raised in rabbit (1:1,000–1:2,000) and antibodies directed either against GAD65 (1:100), or substance P (1:200) or AChE (1:250–1:1,000) followed by a mixture of fluorescein-conjugated sheep antirabbit Ig (1:100) (Silenus Amrad Biotech Borona, Victoria, Australia) and CY3-conjugated goat antimouse Ig (1:100) (Jackson ImmunoResearch, Westgrove PA) or CY3-conjugated goat anti-rat Ig (1:100) (Chemicon).
2. For the dual immunostaining of calretinin/GAD67 or calretinin/GABA, simultaneous incubation with calretinin antibody raised in goat (1:400) and anti-GAD67 (1:1,000) or anti-GABA (1:100), followed by fluorescein isothiocyanate (FITC)-linked donkey antigoat (1:100) (Nordic, Tilburg, Netherlands) and Texas Red-linked donkey antirabbit (1:100) (Amersham, Little Chalfont, UK) as secondary antibodies.

Triton X-100 was omitted when GAD65 and GAD67 immunocytochemistry was used to localize neuronal cell bodies instead of terminals (Esclapez et al., 1994).

Sections processed for double immunohistochemical staining were examined under a Leica TCS 4D confocal scanning laser microscope equipped with an argon-krypton laser and appropriate filter sets for detection of FITC, CY3, and Texas Red. Objectives used were 16, 40, and 100 \times . Images of double-labeled sections were sequentially captured, and then corresponding images were merged by using Adobe Photoshop v.5.0 (San Jose, CA).

Fig. 2. Immunolabeling for calretinin (CR) and substance P (SP) in the target layers of the SUM-hippocampal projections, in coronal sections of the developing (E127, A–D; P12, E and F) and mature monkey hippocampus (G). **A:** Two concentric bands (arrows) of CR immunoreactivity, one thin and dense and the other larger and more lightly stained, extend along the dentate (DG) granular layer (gl) still predominating laterally. Mol, molecular layer. A group of calretinin-labeled fibers is clearly visible in the pyramidal cell layer of CA2. **B:** The intensively labeled terminals in the dentate juxta-granular layer sweep between the somata of the granule cells layer (gl). More dispersed short axonal segments and terminals form the lighter concentric band (arrow) located in the inner one-third of the dentate molecular layer (ml). The calretinin-immunoreactive cell bodies and processes, at the upper limit of the molecular layer (bottom of the figure), are mainly Cajal-Retzius cells. **C:** A thin network of SP immunoreactivity that is denser laterally, is present in the dentate juxtgranular layer (arrows). The overall SP innervation of the Ammon's horn has greatly increased. gl, granular layer. **D:** The paucity of SP-labeled terminals in the dentate outermost granular and juxtgranular layers clearly appears at higher magnification. gl, granular layer; ml, molecular layer. **E:** Postnatal day 12 (P12). A dense but still narrow network of SP-labeled innervation is seen in the dentate outermost granular and juxtgranular layers. Another band of dense SP-positive innervation has developed in the outer half of the molecular layer (oml). gl, granular layer. **F,G:** P12 and 4-year-old adult. The CR-labeled innervation in the dentate molecular layer progressively forms a much larger and denser band than the juxtgranular SP-positive innervation. Scale bars = 100 μ m in A,C; 30 μ m in B,D–G.

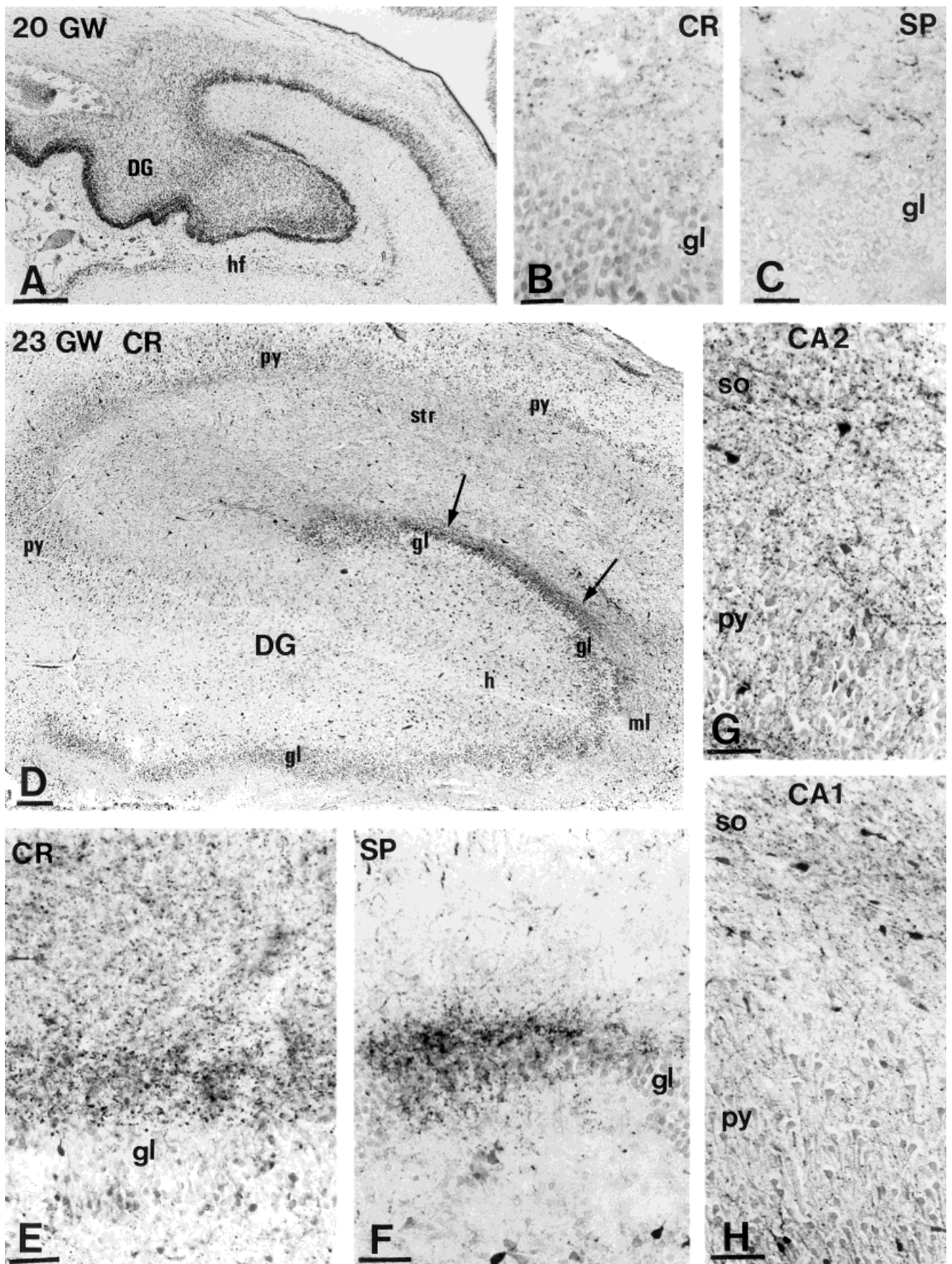


Figure 3

RESULTS

We considered as SUM-hippocampal projections the hippocampal afferents meeting the aforementioned topographical and neurochemical criteria established in the adult monkey (Nitsch and Leranath, 1993, 1994; Seress et al., 1993; Leranath and Nitsch, 1994). The developmental time course in monkey and human fetuses of calretinin and substance P immunoreactivity in the dentate juxtgranular layer and in the CA2 pyramidal cell layer and the co-localization studies intended to specify further the neurochemical nature of the SUM projections will be reported later.

Dentate and ammonic targets of the SUM projections

Development of calretinin- and substance P-positive terminal innervations in the fetal cynomolgus monkey

E88. Numerous calretinin- and substance P-labeled cell bodies and axons were present in Ammon's horn and subiculum (Fig. 1A,B), but the terminals did not display, at any rostrocaudal level of the hippocampus, the characteristic distribution of calretinin- and substance P-immunoreactive terminals in the DG and CA2 subfield described as the targets of the SUM projections in the adult.

E109. A thin band of calretinin-immunoreactive puncta occupied the innermost part of the DG molecular layer (Fig. 1C,E). At the caudal level, where they predominated, they were distributed in both the lateral limb and the crest but appeared only in the lateral limb at the midbody level. A few thin fibers and axon terminals were visualized in the pyramidal cell layer of CA2 (Fig. 1D). A modest accumulation of substance P-containing terminals was also observed in the juxtgranular layer of the dentate lateral limb, predominating caudally (Fig. 1F,G). In contrast, a rich substance P-labeled innervation characterized the whole Ammon's horn, prominent in the pyramidal cell layer and the stratum radiatum of CA2 (Fig. 1F) where it was more abundant than the calretinin-labeled afferents (compare Fig. 1F with C,D).

E127. Deeply stained calretinin-labeled terminals accumulated in the juxtgranular layer of the DG, extending from the lateral to the medial limb, at both midbody and caudal levels (Fig. 2A,B). A network of calretinin-labeled fibers and puncta swept between the somata of granule cells in the most superficial part of the granule cell layer (Fig. 2B). More dispersed short axonal segments and terminals occupied the inner third of the DG molecular layer, forming a pale band of immunoreactivity concentric to the granule cell layer (Fig. 2A,B). The density of calretinin-containing terminals and preterminals increased significantly in the pyramidal cell layer of CA2, slightly extending into the stratum radiatum (Fig. 2A). Substance P-positive terminals still predominated laterocaudally but also reached the medial limb of the DG. Their density slightly increased in the juxtgranular and the outermost granular layers of the DG, but they formed only a thin bundle compared with the calretinin-labeled terminals (Fig. 2C,D). An extremely dense substance P-immunoreactive innervation was present in CA2.

E142 to P12 and adulthood. The substance P- and calretinin-labeled innervations increased in density but displayed the same pattern of distribution as earlier (Fig. 2E-G). The distinctly distributed calretinin innervation along the granule cell layer of the DG constituted progressively from E142 to adulthood a very dense band occupying the inner third or more of the DG molecular layer (Fig. 2F,G). The group of calretinin-labeled terminals in the pyramidal cell layer and stratum radiatum of CA2 also appeared denser and extended into the pyramidal cell layer of CA3. On the other hand, the substance P-labeled innervation observed in the outermost granular and juxtgranular layers of the DG remained a narrow network (Fig. 2E). Another population of substance P-positive terminals accumulated progressively in the outer half of the dentate molecular layer from E142 on, separated by a light band of the substance-P positivity in the juxtgranular layer (Fig. 2E). Hence, there was no substance P-positive equivalent of the wide calretinin-immunoreactive innervation present in the inner third of the dentate molecular layer. All the ammonic fields displayed a high density of substance P terminals.

Development of calretinin and substance P-containing terminal innervations in the human fetal dentate and ammonic targets

17.5 GW. In the few sections available, neither calretinin- or substance P-labeled terminals were observed in the granular or juxtgranular layers of the DG.

20 GW. Calretinin- and substance P-containing varicosities were observed mainly in the DG at the caudal level. They were distributed in the molecular layer of the most lateral limb (Fig. 3A-C). A few calretinin-immunoreactive dots were also scattered in the deep pyramidal cell layer of CA2, whereas substance P-labeled dots were present in the pyramidal cell layer of CA3-CA2.

23-24 to 32.5 GW. Small fibers and terminals labeled for calretinin and substance P accumulated successively in the lateral and then in the medial part of the DG juxtgranular and upper granular cell layers (Fig. 3D-F) at both the caudal pole and the midbody level. An accumulation of calretinin-containing terminals was observed in all layers of the CA2 field (Fig. 3G), contrasting with the poor innervation present in the pyramidal cell layer and stratum radiatum of CA1 (Fig. 3H). Substance-P-

Fig. 3. Labeling patterns of calretinin (CR) and substance P (SP) in the target layers of the SUM-hippocampal projections, in coronal cryostat sections of human fetal hippocampus at 20 (A-C) and 23 (D-H) gestational weeks (GW). **A:** Nissl staining of the hippocampal formation at a caudal level. DG, dentate gyrus; hf, hippocampal fissure. **B:** CR-labeled dots are scattered in the dorso-lateral part of the dentate supragranular layer. Methylene green counterstaining. gl, granular layer. **C:** SP-labeled terminals in the same area. gl, granular layer. **D:** The granular cell layer (gl) of the dentate gyrus (DG) and the pyramidal cell layer (py) of the ammonic fields are visualized by methylene green counterstaining. The dense band of CR-labeled terminals located in the juxtgranular layer of the dentate dorso-lateral limb (arrows) presumably represents the SUM afferents. CR-labeled nonpyramidal neurons are scattered in the DG molecular layer (ml) and hilus (h), and in the stratum radiatum (str) of the ammonic fields. **E:** CR-containing terminals are present in the whole thickness of the dentate molecular layer but clearly accumulate in the juxtgranular cell layer. gl, granular cell layer. **F:** Same area. SP-positive terminals in the dentate granular and juxtgranular layers. gl, granular layer. **G:** CA2 area. The density of CR-labeled terminals in this target area of SUM afferents contrasts with their paucity in CA1, shown in H. so, stratum oriens; py, pyramidal cell layer. **H:** CA1 area. CR immunoreactivity. Methylene green counterstaining. Scale bars = 400 μ m in A; 20 μ m in B,C; 100 μ m in D; 30 μ m in E,F; 40 μ m in G,H.

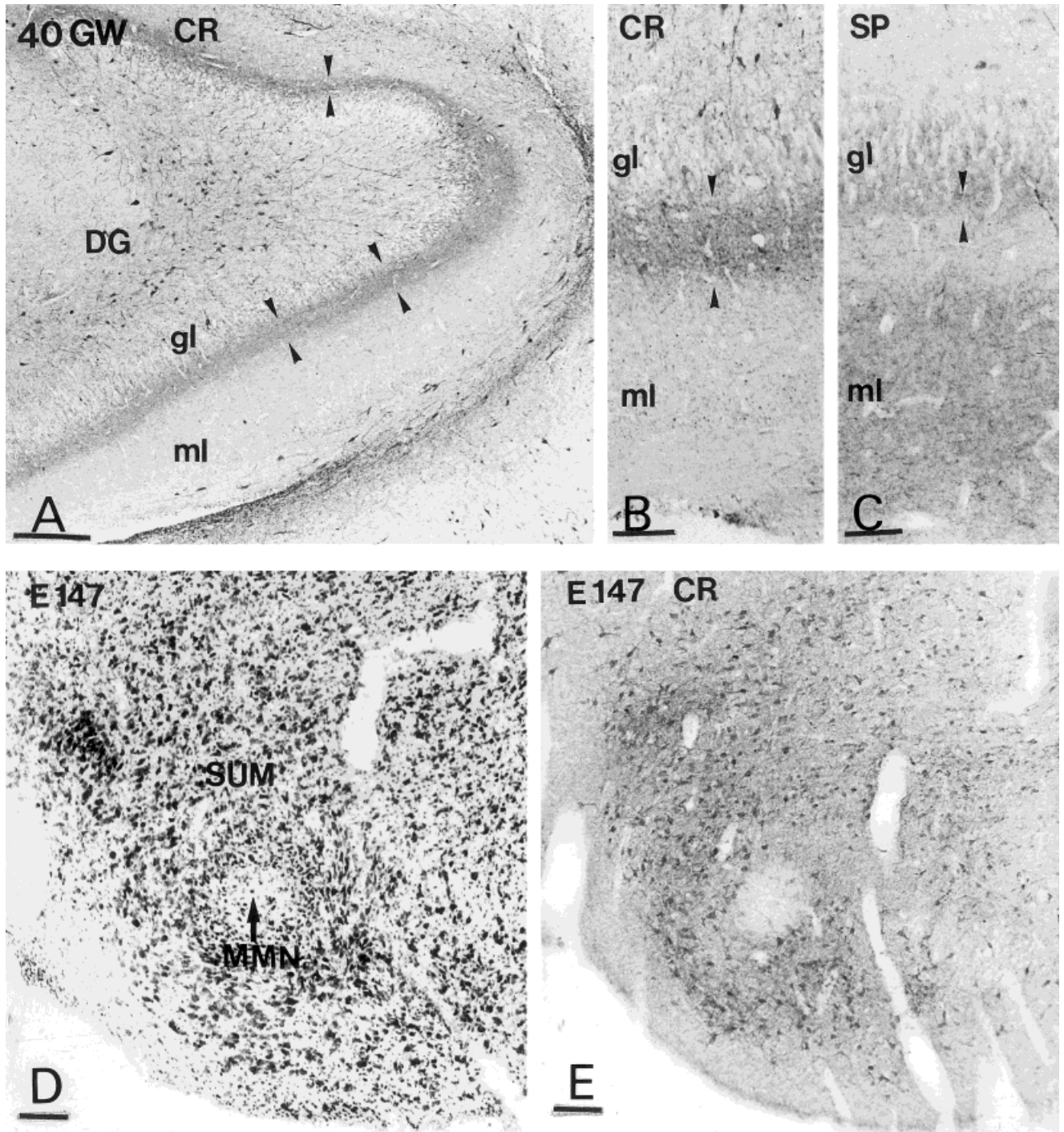


Fig. 4. A–C: Calretinin (CR) and substance P (SP) labeling in paraffin sections of human fetal hippocampus at 40 gestational weeks (GW). **A:** Calretinin-(CR) labeled innervation (arrowheads) in the supra-granular layer of the lateral limb of the dentate gyrus (DG). gl, granular layer; ml, molecular layer. **B:** The juxtargranular CR-immunoreactive innervation (arrowheads) extends into approximately the deep quarter of the dentate molecular layer (ml). gl, granular layer. **C:** The band of SP-labeled terminals in the juxtargranular layer (arrowheads) is much narrower than the CR-labeled

one. As in monkey, it is separated by a light space from a superficial SP innervation in the outer part of the molecular layer (ml). **D, E:** Coronal sections of monkey supramammillary area (SUM) at E 147. **D:** Caudal level with Nissl staining. Medial mammillary nucleus (MMN) at its most caudal part. Midline is on the left. **E:** Consecutive section showing CR immunoreactivity. Numerous CR-containing neurons are observed in the SUM area. Scale bars = 200 μm in A; 50 μm in B,C; 100 μm in D,E.

immunoreactive dots predominated in the pyramidal cell layer of CA3–CA2 but were also seen in CA1.

40 GW versus young and adult brains. At 40 GW, the calretinin- and substance P-containing terminals present in the human DG displayed the same distinct pattern of distribution as that observed in the monkey. Calretinin-labeled terminals formed a dense band in the inner one-fourth of the DG molecular layer and the uppermost granular cell layer (Fig. 4A,B). Numerous positive varicosities were also present in the pyramidal cell layer of CA2 and CA3. The network of substance P-immunoreactive innervation in the juxtgranular layer was narrower than the calretinin-labeled band of terminals, and it was separated by a light space from another large network of substance P-labeled fibers and terminals present in the outer half of the molecular layer (Fig. 4C).

This pattern of distribution of the calretinin innervation in the dentate molecular layer did not match the adult pattern observed in the few hippocampal sections obtained in the second and fourth decade of life. In these adult cases, the dense accumulation of calretinin terminals was restricted to the juxtgranular layer, in keeping with the profile of distribution previously reported in much older subjects (Nitsch and Ohm, 1995).

Co-localization studies in the DG and ammonic targets of the SUM projections

These studies aimed to specify 1) the co-localization of substance P and calretinin in the SUM-hippocampal terminals located in the dentate and ammonic targets; 2) the respective contribution of GABA-containing and GABA-immunonegative calretinin-labeled terminals to the calretinin innervation; and 3) the relationship between calretinin-immunoreactive and AchE-positive innervations.

Double immunostaining for calretinin and substance P. In the fetal monkey, terminals double-labeled for calretinin and substance P were present from E109 on (Fig. 5A) and became numerous in the juxtgranular and the upper granular cell layers of the DG. In contrast, in the inner third of the DG molecular layer, calretinin-single labeled fibers predominated, as could be expected from the previous single-labeling experiments (see above). The pyramidal cell layer of CA2 also contained three populations made of numerous double-labeled substance P/calretinin-positive large varicosities, beside single-labeled substance P- or calretinin-immunoreactive fibers and terminals (Fig. 5B). In human fetal hippocampus, double-labeled calretinin/substance P-positive varicosities also predominated in the immediate juxtgranular layer of the DG (Fig. 5C). They were observed as soon as the calretinin- and substance P-labeled terminal innervations were detected, by 20 GW.

Double immunostaining for calretinin and GAD65. An antibody raised against the isomer 65 of GAD, the synthetic enzyme of GABA, was used selectively for terminal labeling since previous observations in rodents indicated that it produced substantially greater labeling of GABAergic axon terminals than GAD67 (Esclapez et al., 1994). However, both isoforms are present in all the GABAergic neurons of the hippocampal formation (Sloviter et al., 1996; Jongen-Rêlo et al., 1999).

Terminals labeled for calretinin only were numerous in the dentate granular and juxtgranular layers (Fig. 5D) as well as in the CA2 pyramidal layer. They should cor-

respond to the aforementioned extrinsic afferents that co-expressed calretinin and substance P and originate from non-GABAergic cell bodies in the adult SUM (Nitsch and Leranth, 1993, 1994; Leranth and Nitsch, 1994). Terminals double-labeled for calretinin and GAD as well as GAD single-labeled terminals were also present in the same areas, most probably issuing from the numerous local GABAergic interneurons. Most interestingly, the wide band of calretinin-positive innervation that extended in the inner third of the molecular layer was almost entirely GAD immunonegative, a result that eliminated an origin from local circuit neurons.

In human fetal hippocampus, terminals labeled for calretinin only, for calretinin and GAD, or for GAD only were detected from 20 GW on, with a pattern of distribution similar to that observed in the fetal monkey.

Double immunostaining for calretinin and acetylcholinesterase. From E109 to adulthood, fibers single labeled for AchE were present in all the layers of the dentate gyrus (Fig. 5E,F). Terminals that co-expressed calretinin and AchE were located in the deep supragranular and superficial granular layer of the dentate gyrus, first predominating at the laterocaudal level (E109). However, even in the adult, no AchE positivity was observed in the band of fibers and terminals labeled for calretinin but not for GAD, which extended in the deep one-third of the dentate molecular layer.

Co-localization studies in the SUM area of the fetal monkey

Double immunostaining for calretinin and substance P. In the SUM area, calretinin-containing neurons formed a dense neuronal population encapsulating the mid-rostrorocaudal to caudal levels of the medial mammillary nucleus (Fig. 4D,E), as in the adult monkey (Veazey et al., 1982a,b; Nitsch and Leranth, 1993). Substance P was found co-localized with calretinin only in a small neuronal population of the SUM area (Fig. 6A,B).

Double immunostaining for calretinin and GAD65, GAD67, or GABA. No colocalization was observed with GAD65, GAD67, or GABA in the calretinin-labeled neurons of the SUM, in the sections available at the different ages (E109, E136, E147, and E156), whereas GABA- or GAD-labeled neurons were well identified in the mammillary body (Fig. 6C). In contrast, most of the calretinin-containing neurons were contacted by numerous GAD-immunoreactive terminals (Fig. 6D). Very rarely, these GAD-labeled boutons seemed to contain calretinin.

DISCUSSION

The data obtained in the present study provide evidence for an early prenatal development in both human and nonhuman primates of the hippocampal afferent system originating from the supramammillary nucleus (SUM). This pathway appeared to be neurochemically heterogeneous. Our observations also suggest a parallel development of the septo-SUM pathway. The development of the SUM-hippocampal pathway in human and macaques displayed similarities but also differences, which are discussed below.

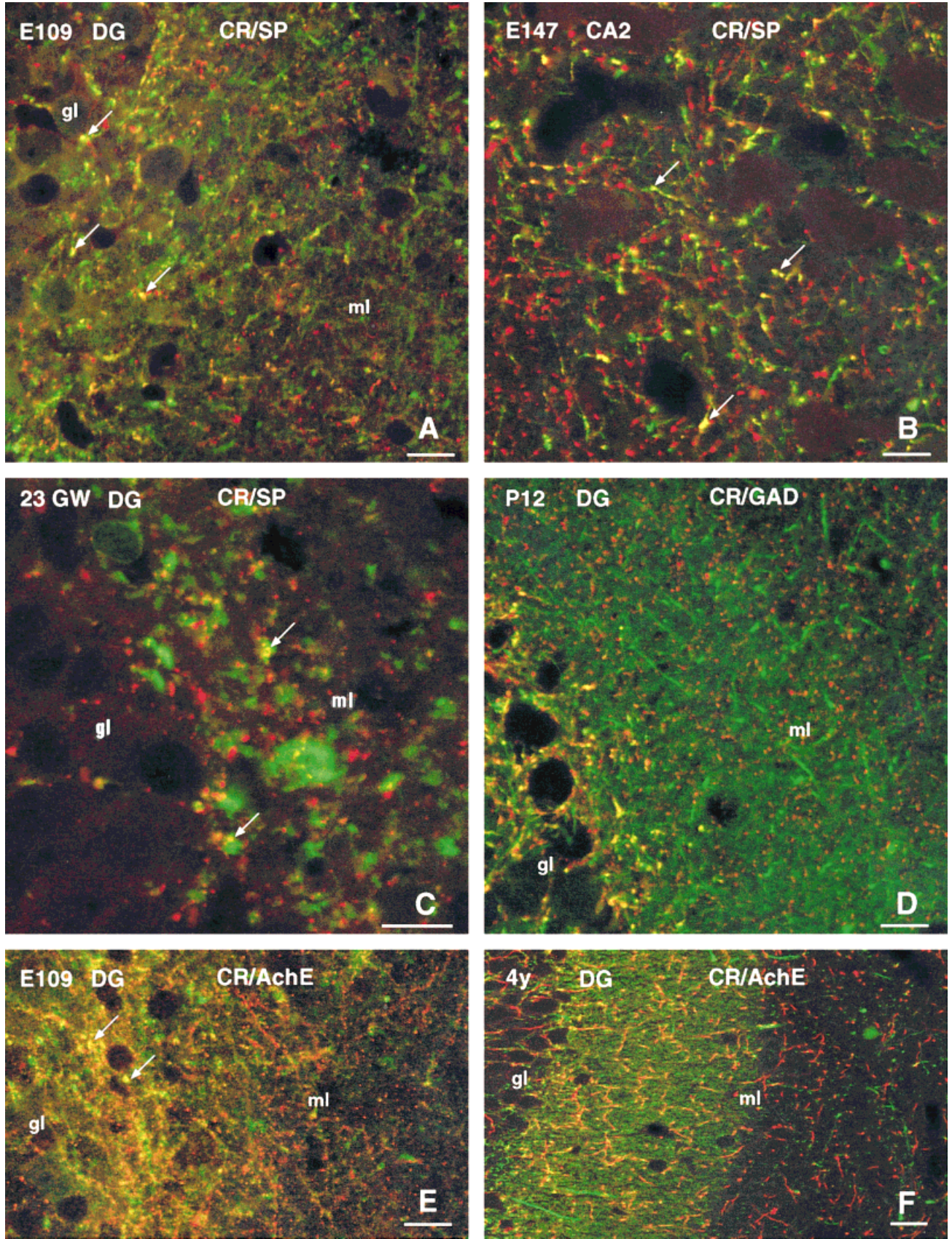


Figure 5

Identification of the developing SUM-hippocampal and septo-SUM projections in human and *Cynomolgus* monkey fetuses

In both human and monkey fetuses, the calretinin- and substance P-labeled terminals, which progressively accumulated in the uppermost granular and deep juxtgranular layers of the dentate gyrus (DG) and in the pyramidal layer and stratum radiatum of CA2, displayed the neurochemical and topographical characteristics of the SUM-hippocampal projections demonstrated in distinct species of adult monkeys and further observed in human adults (Veazy et al., 1982b; Del Fiacco et al., 1987; Sakamoto et al., 1987; Nitsch and Leranthe, 1993, 1994; Seress et al., 1993; Leranthe and Nitsch, 1994; Nitsch and Ohm, 1995). The co-existence of calretinin and substance P immunoreactivity in a large number of these terminals confirmed, at the level of the targets, the previous report of calretinin and substance P co-expression in the parent cell bodies, in the SUM (Nitsch and Leranthe, 1993).

The observation, in dual-labeling experiments, of a basket-like termination of GAD-immunoreactive boutons around the calretinin-labeled neurons of the SUM is in agreement with the data obtained by Borhegyi and Freund (1998) and Leranthe et al. (1999) in rodents.

This large GABAergic innervation might reflect, as in rodents, the arrival of a GABA-containing feedback pathway from the septum to the SUM. However, this should be confirmed by tracing studies.

Neurochemical heterogeneity of the contingent of SUM neurons projecting to the hippocampus? Interspecific differences? A subpopulation of the axon terminals located in the dentate and CA2 target areas of the SUM afferents was immunoreactive either for calretinin or substance P but did not contain both markers. It probably originated from the local calretinin- or substance P-containing GABAergic interneurons of the hippocampus. Numerous terminals containing both calretinin and GAD were indeed observed in these areas, whereas nei-

ther GAD or GABA could be detected in the calretinin-immunoreactive neurons of the SUM in the fetal monkey, in agreement with the observations reported in the adult (Nitsch and Leranthe, 1993).

The origin of the calretinin-labeled innervation that was not labeled with GAD or substance P and extended into the inner third of the dentate molecular layer, beyond the band of calretinin and substance P co-expressing terminals issued from the SUM, was more puzzling. Several possibilities can be considered, implying either an intrinsic or an extrinsic pathway. An origin from local GABAergic neurons seemed unlikely since these fibers were not GAD immunoreactive, whereas almost all calretinin-immunoreactive cells of the monkey hippocampal formation are considered to be GABAergic (Nitsch and Leranthe, 1993; Seress et al., 1993). However, this last point should be further confirmed by the localization of GAD mRNAs.

An origin from the non-GABAergic mossy cells that also project to the inner third of the dentate molecular layer (Buckmaster et al., 1996) also seemed unlikely, since they are not calretinin positive in primates (Seress et al., 1993; Nitsch and Ohm, 1995). Another possibility could be that these fibers originated from a subset of SUM calretinin-containing neurons that did not express substance P. Favoring this hypothesis, only a small proportion of the calretinin-labeled neurons located in the SUM of the fetal *Cynomolgus* monkey were immunoreactive for substance P. This finding, which was at variance with the data reported in the adult monkey (Nitsch and Leranthe, 1993; Seress et al., 1993), might be explained by the impossibility of using colchicine injections in this study to facilitate the cell body immunostaining of these long projecting peptidergic neurons. On the other hand, since these authors did not observe in the African green monkey the extended calretinin innervation present through fetal life to adulthood in the *Cynomolgus* monkey, one can question the presence of interspecific differences. In fact, such a difference has already been demonstrated between the African green monkey and the rat since in the latter species, calretinin and substance P are contained in two distinct subsets of SUM-hippocampal projections (Borhegyi and Leranthe, 1997).

Searching for another argument favoring the SUM origin of this extended calretinin, non-GABAergic innervation, we looked for a co-localization with AchE, since this enzyme is expressed in the SUM neurons projecting to the hippocampus (Bakst and Amaral, 1984). As expected, the double immunostaining procedure used in the present study revealed the co-existence of calretinin and AchE immunoreactivity. However, the double-labeled terminals observed in the dentate gyrus were restricted to the outermost granular and juxtgranular layers. Hence, the origin of the dense calretinin-positive innervation located in the inner third of the dentate molecular layer, which contained neither substance P nor GABA nor AchE, remains an open question.

Parallel developmental temporal profile of the SUM projections and their dentate and ammonic targets in macaques

The SUM-hippocampal afferents reached the dentate gyrus and CA2 field at two-thirds of gestation and increased rapidly in density until the postnatal period. This prenatal development paralleled that of their targets,

Fig. 5. Confocal micrographs of coronal sections of monkey and human fetal brain. A–C: Double immunostaining for calretinin (CR, in green) and substance P (SP, in red). **A:** E 109, dentate gyrus (DG). CR/SP double-labeled (yellow) varicosities (arrows) are present in the juxtgranular layer. gl, granular layer; ml, molecular layer. **B:** E147, CA2 area. Numerous CR/SP double-labeled (yellow) varicosities (arrows) are present in the pyramidal cell layer. **C:** Human fetus, 23 gestational weeks (GW). Dentate gyrus. CR/SP double-labeled (yellow) varicosities (arrows) are present in the outermost granular and juxtgranular cell layers. gl, granular layer. ml, molecular layer. **D:** P12, dentate gyrus. Simultaneous immunostaining for CR (in green) and GAD (in red). The large band of CR-reactive fibers in the deep one-third of the dentate molecular layer and many terminals in the juxtgranular layer are not GAD-immunoreactive and should correspond to extrinsic afferents partly from the SUM. The CR/GAD double-labeled (yellow) varicosities observed in the juxtgranular layer could originate from local GABAergic neurons containing CR. gl, granular layer; ml, molecular layer. **E, F:** Simultaneous immunostaining for CR (in green) and acetylcholinesterase (AChE, in red). **E:** E109, dentate gyrus. CR/AChE double-labeled (yellow) varicosities (arrows) are numerous in the juxtgranular layer. They probably correspond to terminal afferents from the SUM. gl, granular layer; ml, molecular layer. **F:** A 4-year-old adult monkey, dentate gyrus. The CR-positive innervation (green) in the deep one-third of the dentate molecular layer is not AchE immunoreactive. gl, granular layer; ml, molecular layer. Scale bars = 10 μm in A–E; 20 μm in F.

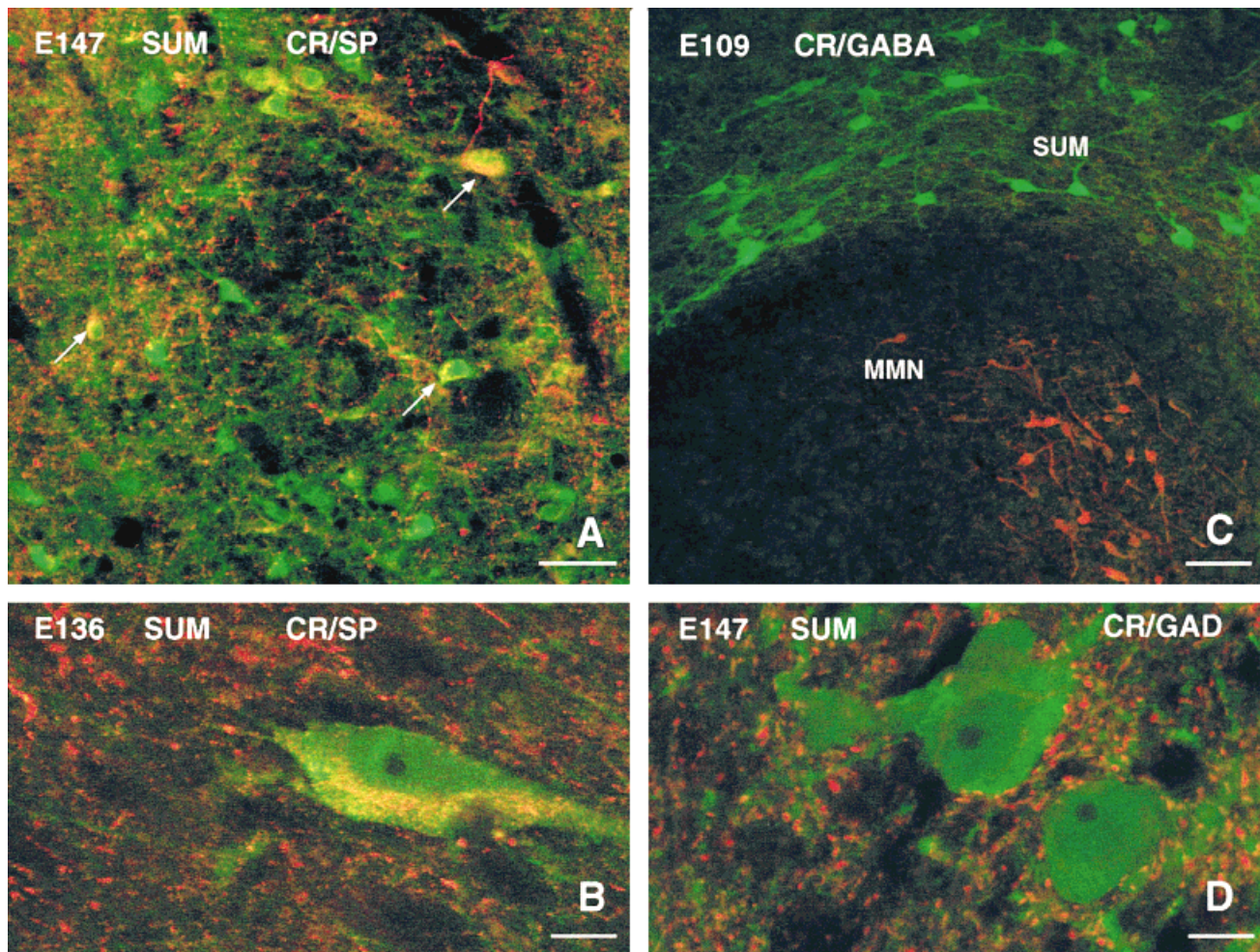


Fig. 6. Coronal sections of the SUM area. Simultaneous detection of calretinin (CR, in green) and substance P (SP, in red). **A:** E147. Among the large number of CR-immunoreactive neurons, a relatively small population (arrows) co-expresses SP (yellow inclusions). **B:** E136. High magnification of a SUM neuron double-labeled for CR and SP. **C:** E109. Many γ -aminobutyric acid (GABA)ergic neurons (in

red) are present in the medial mammillary nucleus (MMN), but the CR-labeled neurons (in green) in the SUM area are not GABA immunoreactive. **D:** E147. Numerous GAD-labeled terminals (in red) of presumed septo-SUM afferents contact CR-immunoreactive neurons (in green). Scale bars = 50 μ m in A,C; 10 μ m in B,D.

principal cells, and specific subpopulations of nonpyramidal local circuit neurons (Nitsch and Leranth, 1993, 1994; Seress et al., 1993; Leranth and Nitsch, 1994).

In the dentate gyrus, the granule cells of the multiple primary dendrite type, which are the most differentiated at all developmental stages (Duffy and Rakic, 1983), have their somata closer to the molecular layer, i.e., closer to the band of SUM terminals located in the uppermost granular and juxtgranular layers. They bear the highest density of spines. These are present on granule cell dendrites from E95 on and increase 12-fold from E95 to birth, on the proximal dendritic segment in the inner molecular layer (Duffy and Rakic, 1983). Moreover, asymmetrical synapses are the first to appear and their density increases sharply during the last one-third of gestation (Eckenhoff and Rakic, 1991), a feature that fits well with the arrival of the SUM excitatory afferents. In the hippocampus proper, the pyramidal cells of CA2 displayed an advanced level of dendritic and spine differentiation by two-thirds of gestation (personal observations).

Finally, previous studies have also provided evidence for early prenatal development and maturation of the different populations of GABAergic neurons (Berger and Alvarez, 1996; Berger et al., 1999; Esclapez et al., 1999) that are targeted by the SUM-hippocampal projections (Leranth and Nitsch, 1994) besides the principal neurons. The basket cells in particular, whose rhythmic discharge in the adult brings about the theta-related rhythmic hyperpolarization of principal cells (Cobb et al., 1995; Ylinen et al., 1995), form synaptic contacts in fetal monkey hippocampus by two-thirds of gestation (Berger et al., 1999). During the late prenatal period, we did observe perisomatic and peridendritic innervation of parvalbumin-positive basket cells by substance P-labeled terminals, as described in the adult monkey DG (Leranth and Nitsch, 1994). Together, these data suggest that the SUM-hippocampal afferents establish synaptic contacts with their targets during the second half of gestation. A strong argument supporting this hypothesis was provided by patch-clamp recordings realized in fetal monkey hip-

poampal slices. They have demonstrated the occurrence of functional glutamatergic synapses on hippocampal neurons at the same developmental stages (Khazipov et al., 1999).

Similarities and differences between macaques and humans regarding the SUM-hippocampal pathway

SUM-hippocampal afferents were identified in human fetuses by using the same criteria as in monkeys and displayed a similar developmental profile. However, two main differences were observed. First, they reached the DG and CA2 field earlier in human than in fetal macaques, by midgestation versus two-thirds of gestation. This more precocious temporal profile of development was nevertheless parallel to that of the ammonic targets as in the monkey. Apical dendrites of pyramidal neurons in the ammonic fields have been reported to exhibit morphological characteristics of rapid growth and differentiation as early as 15–18 weeks of gestation in humans (Paldino and Purpura, 1979), an age when they already bear a few asymmetric synapses (Kostovic et al., 1989). α -Amino-3-hydroxy-5-methyl-4-isoxazole-propionic acid (AMPA), N-methyl-D-aspartate (NMDA), and kainate excitatory amino acid receptors are present in the human fetal hippocampus at the end of the first half of gestation (Represa et al., 1986, 1989; Barks et al., 1988; Lee and Choi, 1992). Thereafter, the differentiation of the pyramidal cells follows a caudal to rostral and lateral to medial gradient similarly to the SUM afferents, with a maximal phase of development of CA2 and CA3 pyramidal cells occurring by the last one-third of gestation (Paldino and Purpura, 1979; Arnold and Trojanowski, 1996a).

A second main difference was the disappearance in young or older adults (Nitsch and Ohm, 1995; present study) of the extended band of calretinin innervation present in human and monkey fetuses, in the inner third of the dentate molecular layer. These interspecific differences between monkey and human hippocampal formation are not unique features since another recently described hippocampal pathway, "the endfolial fiber pathway," seems to be unique to humans (Lim et al., 1997).

Functional considerations

In rodents, most of the calretinin-immunoreactive neurons of the SUM-hippocampal system are aspartate/glutamatergic (Kiss et al., 2000). Similar data are not available in primates, but they are in line with the lack of GABA and GAD immunoreactivity in the calretinin-containing neurons of the SUM in fetal and adult monkeys and the asymmetrical synapses formed by their terminals (Seress et al., 1993; Leranth and Nitsch, 1994). Excitatory amino acids are considered to serve a neurotrophic function and to participate in the formation of hippocampal neuronal circuitry (for review, see Mattson et al., 1988; McDonald and Johnston, 1990; Diabira et al., 1999). This role has been recently specified by the finding that a positive modulation of AMPA receptors is able to cause rapid and substantial increases in neurotrophin expression (brain-derived neurotrophic factor [BDNF] and to a lesser extent nerve growth factor [NGF]) (Lauterborn et al., 2000). In keeping with the early arrival of the perforant path issued from the entorhinal cortex (Arnold and Trojanowski, 1996b; Hevner and Kinney, 1996), this glu-

tamatergic transmission may play an important role in the activity-dependent development of the fetal primate hippocampal formation. On the other hand, SUM terminals contact not only principal cells but also specific subpopulations of nonpyramidal cells, a feature suggesting a complex effect on the signal flow (Leranth and Nitsch, 1994).

The developing SUM-hippocampal glutamatergic system may contribute to the induction of theta-like activity patterns similar to those obtained by positive modulation of hippocampal AMPA receptors (Lauterborn et al., 2000). Both theta rhythmic waves and membrane potential oscillations, generated in the theta frequency range, have been reported to occur in rat pups at the end of the first postnatal week (Leblanc and Bland, 1979; Konopacki et al., 1988; Strata, 1998) or even earlier (Psarropoulou and Avoli, 1995). Unfortunately, morphological data on the pre- or early postnatal development of the SUM-hippocampal projections in rodents are not available. However, since several events that take place during the first postnatal week in rats are already detected during prenatal life in primates, for instance the development of basket cells (Berger et al., 1999) or the generation of slow network-driven oscillations such as giant depolarizing potentials (Khazipov et al., 1999), the hypothesis of an in utero development of theta-like activity in primates deserves detailed analyses in future studies.

In conclusion, a body of convergent morphological, neurochemical, and electrophysiological data, including the development of functional GABAergic and glutamatergic synapses (Berger and Alvarez, 1996; Berger et al., 1999; Esclapez et al., 1999; Khazipov et al., 1999), strongly suggests that an important part of the mature hippocampal circuitry develops relatively fast and starts to be functional by two-thirds of gestation in macaques and perhaps earlier in humans. It represents an essential morphofunctional support for the elaboration of the mnemonic capacities demonstrated in human and nonhuman neonates (Bachevalier et al., 1993; Bachevalier and Mishkin, 1994; Pascalis and de Schonen, 1994; Pascalis and Bachevalier, 1999). The data obtained in the present study also provide additional support for the view that the fetal macaque is a valid model for the human hippocampal prenatal development. However, the subtle differences observed between the two species, in keeping with other recently reported unexpected differences (Lim et al., 1997), stress the need for further comparative studies.

ACKNOWLEDGMENTS

The authors thank Dr. G. Germain for performing the cesarean sections in monkeys at the Primate Center of the Institut National de la Recherche Agronomique, Dr. P. Gaspar for helpful comments, C. Nze for assistance with the confocal laser scanning, and D. Le Cren for expert photographic work.

LITERATURE CITED

- Alonso JR, Amaral DG. 1995. Cholinergic innervation of the primate hippocampal formation. I. Distribution of choline acetyltransferase immunoreactivity in the *Macaca fascicularis* and *Macaca mulatta* monkeys. *J Comp Neurol* 355:135–170.
- Arnold SE, Trojanowski JQ. 1996a. Human fetal hippocampal development. I. Cytoarchitecture, myeloarchitecture and neuronal morphological features. *J Comp Neurol* 367:274–292.

- Arnold SE, Trojanowski JQ. 1996b. Human fetal hippocampal development. II. The neuronal cytoskeleton. *J Comp Neurol* 367:293–307.
- Bachevalier J, Mishkin M. 1994. Effects of selective neonatal temporal lobe lesions on visual recognition memory in rhesus monkeys. *J Neurosci* 14:2128–2139.
- Bachevalier J, Brickson M, Hagger C. 1993. Limbic-dependent recognition memory in monkeys develops early in infancy. *Neuroreport* 4:77–80.
- Bakst I, Amaral DG. 1984. The distribution of acetylcholinesterase in the hippocampal formation of the monkey. *J Comp Neurol* 225:344–371.
- Barks JD, Silverstein FS, Sims K, Greenamyre JT, Johnston MV. 1988. Glutamate recognition sites in human fetal brain. *Neurosci Lett* 84:131–136.
- Berger B, Alvarez C. 1996. Neurochemical development of the hippocampal region in the fetal rhesus monkey. III. Calbindin-D28K, calretinin and parvalbumin, with special mention of Cajal-Retzius cells and the retrosplenial cortex. *J Comp Neurol* 366:674–699.
- Berger B, Alvarez C, Pelaprat D. 1997. Retrosplenial/presubicular continuum in primates: a developmental approach in fetal macaques using neurotensin and parvalbumin as markers. *Brain Res Dev Brain Res* 101:207–224.
- Berger B, De Grissac N, Alvarez C. 1999. Precocious development of parvalbumin-like immunoreactive interneurons in the hippocampal formation and entorhinal cortex of the fetal cynomolgus monkey. *J Comp Neurol* 403:309–331.
- Bland BH, Oddie SD. 1998. Anatomical, electrophysiological and pharmacological studies of ascending brainstem hippocampal synchronizing pathways. *Neurosci Biobehav Rev* 22:259–273.
- Borhegyi Z, Freund TF. 1998. Dual projection from the medial septum to the supramammillary nucleus in the rat. *Brain Res Bull* 46:453–459.
- Borhegyi Z, Leranath C. 1997. Distinct substance P- and calretinin-containing projections from the supramammillary area to the hippocampus in rats; a species difference between rats and monkeys. *Exp Brain Res* 115:369–374.
- Buckmaster PS, Wenzel HJ, Kunkel DD, Schwartzkroin PA. 1996. Axon arbors and synaptic connections of hippocampal mossy cells in the rat in vivo. *J Comp Neurol* 366:270–292.
- Chang Y-C, Gottlieb DI. 1988. Characterization of the proteins purified with monoclonal antibodies to glutamic acid decarboxylase. *J Neurosci* 8:2123–2130.
- Cobb SR, Buhl EH, Halasy K, Paulsen O, Somogyi P. 1995. Synchronization of neuronal activity in hippocampus by individual GABAergic interneurons. *Nature* 378:75–78.
- Crowne DP, Radcliffe DD. 1975. Some characteristics and functional relations of the electrical activity of the primate hippocampus and a hypothesis of hippocampal function. In: Isaacson RL, Pribram KH, editors. *The hippocampus*, vol 2. New York: Plenum. p 185–205.
- Del Fiacco M, Levanti MC, Dessi ML, Zucca G. 1987. The human hippocampal formation and parahippocampal gyrus localization of substance P-like immunoreactivity in newborn and adult post-mortem tissue. *Neuroscience* 21:141–150.
- Diabira D, Hennou S, Chevassus-au-Louis N, Ben-Ari Y, Gozlan H. 1999. Late embryonic expression of AMPA receptor function in the CA1 region of the intact hippocampus in vitro. *Eur J Neurosci* 11:4015–4023.
- Duffy CJ, Rakic P. 1983. Differentiation of granule cell dendrites in the dentate gyrus of the rhesus monkey: a quantitative Golgi study. *J Comp Neurol* 214:224–237.
- Eckenhoff MF, Rakic P. 1991. A quantitative analysis of synaptogenesis in the molecular layer of the dentate gyrus in the rhesus monkey. *Brain Res Dev Brain Res* 64:129–135.
- Eifuku S, Nishijo H, Kita T, Ono T. 1995. Neuronal activity in the primate hippocampal formation during a conditional association task based on the subject's location. *J Neurosci* 15:4952–4969.
- Esclapez M, Tillakaratne NJK, Kaufman DL, Tobin AJ, Houser CR. 1994. Comparative localization of two forms of glutamic acid decarboxylase and their mRNAs in rat brain supports the concept of functional differences between the forms. *J Neurosci* 14:1834–1855.
- Esclapez M, Dinocourt C, Ben-Ari Y, Berger B. 1999. Developmental changes of GABA interneurons in the fetal hippocampal formation (HF) of the cynomolgus monkey. *Soc Neurosci Abstr* 29:2266.
- Haglund L, Swanson LW, Köhler C. 1984. The projection of the supramammillary nucleus to the hippocampal formation: an immunohistochemical and anterograde transport study with the lectin PHA-L in the rat. *J Comp Neurol* 229:171–185.
- Hevner RF, Kinney HC. 1996. Reciprocal entorhinal-hippocampal connections established by human fetal midgestation. *J Comp Neurol* 372:384–394.
- Holscher C, Anwyl R, Rowan MJ. 1997. Stimulation on the positive phase of hippocampal theta rhythm induces long-term potentiation that can be depotentiated by stimulation on the negative phase in area CA1 in vivo. *J Neurosci* 17:6470–6477.
- Jongen-Rêlo AL, Pitkänen A, Amaral DG. 1999. Distribution of GABAergic cells and fibers in the hippocampal formation of the macaque monkey: an immunohistochemical and in situ hybridization study. *J Comp Neurol* 408:237–271.
- Kahana MJ, Sekuler R, Caplan JB, Kirschen M, Madsen JR. 1999. Human theta oscillations exhibit task dependence during virtual maze navigation. *Nature* 399:781–784.
- Kaufman DL, Houser CR, Tobin AJ. 1991. Two forms of the gamma-aminobutyric acid synthetic enzyme glutamate decarboxylase have distinct intraneuronal distributions and cofactor interactions. *J Neurochem* 56:720–723.
- Khazipov R, Esclapez M, Caillard O, Bernard C, Hirsch J, Leinekugel X, Berger B, Ben-Ari Y. 1999. Early maturation of hippocampal network in the fetal cynomolgus monkey. *Soc Neurosci Abstr* 29:2266.
- Kirk IJ. 1998. Frequency modulation of hippocampal theta by the supramammillary nucleus, and other hypothalamo-hippocampal interactions: mechanisms and functional implications. *Neurosci Biobehav Rev* 22:291–302.
- Kirk IJ, McNaughton N. 1993. Mapping the differential effects of procaine on frequency and amplitude of reticularly elicited hippocampal rhythmic slow activity. *Hippocampus* 4:517–526.
- Kirk IJ, Oddie SD, Konopacki J, Bland BH. 1996. Evidence for differential control of posterior hypothalamic, supramammillary, and medial mammillary theta-related cellular discharge by ascending and descending pathways. *J Neurosci* 16:5547–5554.
- Kiss J, Csaki A, Bokor H, Shanabrough M, Leranath C. 2000. The supramammillo-hippocampal and supramammillo-septal glutamatergic/aspartatergic projections in the rat: a combined (³H)D-aspartate autoradiographic and immunohistochemical study. *Neuroscience* 97:657–699.
- Klimesch W. 1999. EEG alpha and theta oscillations reflect cognitive and memory performance: a review and analysis. *Brain Res Brain Res Rev* 29:169–195.
- Kocsis B, Vertes RP. 1994. Characterization of neurons of the supramammillary nucleus and mammillary body that discharge rhythmically with the hippocampal theta rhythm in the rat. *J Neurosci* 14:7040–7052.
- Konopacki J., Bland BH, Roth SH. 1988. The development of carbachol-induced EEG theta examined in hippocampal formation slices. *Brain Res Dev Brain Res* 38:229–232.
- Kostovic I, Seress L, Mrzljak L, Judas M. 1989. Early onset of synapse formation in the human hippocampus: a correlation with Nissl-Golgi architectonics in 15- and 16.5-week-old fetuses. *Neuroscience* 30:105–116.
- Lauterborn JC, Lynch G, Vanderklish P, Arai A, Gall CM. 2000. Positive modulation of AMPA receptors increases neurotrophin expression by hippocampal and cortical neurons. *J Neurosci* 20:8–21.
- Leblanc MO, Bland BH. 1979. Developmental aspects of hippocampal electrical activity and motor behavior in the rat. *Exp Neurol* 66:220–237.
- Lee HS, Choi BH. 1992. Density and distribution of excitatory amino acid receptors in the developing human fetal brain. A quantitative autoradiographic study. *Exp Neurol* 118:284–290.
- Leranath C, Nitsch R. 1994. Morphological evidence that hypothalamic substance P-containing afferents are capable of filtering the signal flow in the monkey hippocampal formation. *J Neurosci* 14:4079–4094.
- Leranath C, Carpi D, Buzsaki G, Kiss J. 1999. The entorhino-septo-supramammillary nucleus connection in the rat: morphological basis of a feedback mechanism regulating hippocampal theta rhythm. *Neuroscience* 88:701–718.
- Lim C, Mufson EJ, Kordower JH, Blume HW, Madsen JR, Saper CB. 1997. Connections of the hippocampal formation in humans. II. The endfolial fiber pathway. *J Comp Neurol* 385:352–371.
- McDonald JW, Johnston MV. 1990. Physiological and pathophysiological roles of excitatory amino acids during central nervous system development. *Brain Res Brain Res Rev* 15:41–70.
- McNaughton N, Logan B, Panicker KS, Kirk IJ, Pan WX, Brown NT, Heenan A. 1995. Contribution of synapses in the medial supramammillary nucleus to the frequency of hippocampal theta rhythm in freely moving rats. *Hippocampus* 5:534–545.

- Mattson MP, Lee RE, Adams ME, Guthrie PB, Kater SB. 1988. Interactions between entorhinal axons and target hippocampal neurons: a role for glutamate in the development of hippocampal circuitry. *Neuron* 1:865–876.
- Meador KJ, Thompson JL, Loring DW, Murro AM, King DW, Gallagher BB, Lee GP, Smith JR, Flanigin HF. 1991. Behavioral state-specific changes in human hippocampal theta activity. *Neurology* 41:869–872.
- Nitsch R, Leranth C. 1993. Calretinin immunoreactivity in the monkey hippocampal formation. II. Intrinsic GABAergic and hypothalamic non-GABAergic systems: an experimental tracing and co-existence study. *Neuroscience* 55:797–812.
- Nitsch R, Leranth C. 1994. Substance P-containing hypothalamic afferents to the monkey hippocampus: an immunocytochemical, tracing and coexistence study. *Exp Brain Res* 101:231–240.
- Nitsch R, Ohm TG. 1995. Calretinin immunoreactive structures in the human hippocampal formation. *J Comp Neurol* 360:475–487.
- Paldino AM, Purpura DP. 1979. Branching patterns of hippocampal neurons of human fetus during dendritic differentiation. *Exp Neurol* 64:620–631.
- Pascalis O, Bachevalier J. 1999. Neonatal aspiration lesions of the hippocampal formation impair visual recognition memory when assessed by paired-comparison task but not by delayed nonmatching-to-sample task. *Hippocampus* 9:609–616.
- Pascalis O, de Schönen S. 1994. Recognition memory in 3 to 4 day-old human neonates. *Neuroreport* 5:1721–1724.
- Perez Y, Chapman CA, Woodhall G, Robitaille R, Lacaille JC. 1999. Differential induction of long-lasting potentiation of inhibitory postsynaptic potentials by theta patterned stimulation versus 100-Hz tetanization in hippocampal pyramidal cells in vitro. *Neuroscience* 90:747–757.
- Psarropoulou C, Avoli M. 1995. Subthreshold membrane-potential oscillations in immature CA3 hippocampal neurones. *Neuroreport* 6:2561–2564.
- Represa A, Tremblay E, Schoevar D, Ben-Ari Y. 1986. Development of high affinity kainate binding sites in human and rat hippocampi. *Brain Res* 384:170–174.
- Represa A, Tremblay E, Ben-Ari Y. 1989. Transient increase of NMDA-binding sites in human hippocampus during development. *Neurosci Lett* 99:61–66.
- Sakamoto N, Michel JP, Kopp N, Tohyama M, Pearson J. 1987. Substance P- and enkephalin-immunoreactive neurons in the hippocampus and related areas of the human infant brain. *Neuroscience* 22:801–811.
- Saper CB. 1985. Organization of cerebral cortical afferent systems in the rat. II. Hypothalamocortical projections. *J Comp Neurol* 237:21–46.
- Schwaller B, Buchwald P, Blümke I, Celio MR, Hunziker W. 1993. Characterization of a polyclonal antiserum against the purified recombinant calcium-binding protein calretinin. *Cell Calcium* 14:639–648.
- Seress L, Nitsch R, Leranth C. 1993. Calretinin immunoreactivity in the monkey hippocampal formation-I. Light and electron microscopic characteristics and co-localization with other calcium-binding proteins. *Neuroscience* 55:775–796.
- Seress L, Ribak CE. 1995. Postnatal development of CA3 pyramidal neurons and their afferents in the Ammon's horn of rhesus monkeys. *Hippocampus* 5:217–231.
- Sloviter RS, Dichter MA, Rachinsky TL, Dean E, Goodman JH, Sollas AL, Martin DL. 1996. Basal expression and induction of glutamate decarboxylase and GABA in excitatory granule cells of the rat and monkey hippocampal dentate gyrus. *J Comp Neurol* 373:593–618.
- Stewart M, Fox SE. 1991. Hippocampal theta activity in monkeys. *Brain Res* 538:59–63.
- Strata F. 1998. Intrinsic oscillations in CA3 hippocampal pyramids: physiological relevance to theta rhythm generation. *Hippocampus* 8:666–679.
- Swanson LW, Cowan WM. 1979. The connections of the septal region of the rat. *J Comp Neurol* 186:621–656.
- Tesche CD, Karhu J. 2000. Theta oscillations index human hippocampal activation during a working memory task. *Proc Natl Acad Sci USA* 97:919–924.
- Thomas MJ, Watabe AM, Moody TD, Makhinson M, O'Dell TJ. 1998. Postsynaptic complex spike bursting enables the induction of LTP by theta frequency synaptic stimulation. *J Neurosci* 18:7118–7126.
- Veazey RB, Amaral DG, Cowan WM. 1982a. The morphology and connections of the posterior hypothalamus in the cynomolgus monkey (*Macaca fascicularis*). I. Cytoarchitectonic organization. *J Comp Neurol* 207:114–134.
- Veazey RB, Amaral DG, Cowan WM. 1982b. The morphology and connections of the posterior hypothalamus in the cynomolgus monkey (*Macaca fascicularis*). II. Efferent connections. *J Comp Neurol* 207:135–156.
- Vertes RP. 1992. PHA-L analysis of projections from the supramammillary nucleus in the rat. *J Comp Neurol* 326:595–622.
- Vertes RP, Kocsis B. 1997. Brainstem-diencephalo-septohippocampal systems controlling the theta rhythm of the hippocampus. *Neuroscience* 81:893–926.
- Watanabe T, Niki H. 1985. Hippocampal unit activity and delayed response in the monkey. *Brain Res* 325:241–254.
- Werner M, Wasielewski R von, Komminoth P. 1996. Antigen retrieval, signal amplification and intensification in immunohistochemistry. *Histochem Cell Biol* 105:253–260.
- Ylinen A, Soltész I, Bragin A. 1995. Intracellular correlates of hippocampal theta rhythm in identified pyramidal cells, granule cells, and basket cells. *Hippocampus* 5:78–90.